Bis(dioxolene)(bipyridine)ruthenium Redox Series

A. B. P. Lever,* Pamela R. Auburn, Elaine S. Dodsworth, Masa-aki Haga,[1a] Wei Liu,[1b] Milan Melnik,[1c] and W. Andrew Nevin[1d]

Contribution from the Department of Chemistry, York University, North York (Toronto), Ontario, Canada M3J 1P3. *Received February 16, 1988*

Abstract: Complexes of the general formula $[Ru(bpy)(dioxolene)_2]^{n+}$ have been prepared where (bpy) is 2,2′-bipyridine and $n = -1, 0, +1$. The dioxolene ligand is 1,2-dihydroxybenzene (catechol), 3,5-di-*tert*-butyl- or 3,4,5,6-tetrachloro-1,2-dihydroxybenzene which may formally exist in the catecholate, semiquinone, or quinone oxidation state. Redox series of up to five members have been prepared by controlled potential electrolysis of the parent species or, in some cases, by chemical oxidation or reduction. Electrochemistry, magnetism, X-ray structural data and ultraviolet, visible and near infrared electronic, resonance Raman, vibrational (FTIR), nuclear magnetic resonance, electron spin resonance and photoelectron spectra, for various members of the redox series, are discussed in terms of the electronic structures (effective oxidation states, delocalization) of the complexes. Apparent conflicts between results obtained with different techniques are resolved by using a simple, qualitative MO model.

The concept of oxidation state is central to the understanding of inorganic chemistry. For covalently bonded substances, the oxidation state concept is a formalism based on conventions which enables the categorization of chemical behavior and physical properties. These conventions break down in coordination complexes with extensive delocalization, such as the dithiolenes.[2] In such cases the oxidation state may no longer be defined as an integer, and the chemical properties are more easily explained with a molecular orbital model. Such delocalization was not thought to occur in dioxolene complexes[3] but is shown to occur to a significant extent in the ruthenium complexes described here.

Metal complexes containing dioxolene ligands (dioxo members of the catechol–quinone redox series) have been the subject of many recent publications.[3-33] The placing of two "noninnocent" ligands on one central metal ion, which itself is redox-active, provides useful insight into metal–ligand bonding, intramolecular electron transfer, and the concept of oxidation state in coordination chemistry.

We have recently reported electrochemical and spectroscopic data for a redox series based upon $Ru(bpy)_2$(dioxolene) and $Ru(py)_4$(dioxolene) where the dioxolene ligand was in the catechol, semiquinone, or quinone oxidation state.[4] Electrochemical and spectroscopic data were presented to show that the ruthenium could be regarded as Ru(II) throughout this series but that some delocalization occurred in the two oxidized species.[4,5] We describe here Ru(bpy)(dioxolene)$_2$ species where dioxolene is derived from 1,2-dihydroxybenzene (catechol, $CatH_2$), 3,5-di-*tert*-butyl- ($DTBCatH_2$), or 3,4,5,6-tetrachloro-1,2-dihydroxybenzene ($TClCatH_2$).

The characterization of the oxidation states of the various components (dioxolene ligands and metal) of these molecules presents difficulties; the electronic structures are not obvious from the molecular formulas. The two dioxolene ligands have a total of six accessible oxidation states, three for each ligand, and the ruthenium could be in the (II), (III), or (IV) oxidation state, giving nine possible combinations. Upon initial examination the various experimental techniques lead to conflicting conclusions, but it is shown that, by using a simple, qualitative MO model, the data can be rationalized in terms of fairly well defined but delocalized electronic structures.

Problems in assigning oxidation states have been encountered in Ru and Os ammines containing ligands with very low-energy π^* orbitals which mix strongly with one of the metal d orbitals.[34,35] Some Os complexes, which formally contain metal(II), show charge-transfer bands in their electronic spectra which behave like ligand-to-metal charge transfer (L → Os(III)), and the $[Ru^{II}(NH_3)_5(N\text{-methylpyrazinium})]^{3+}$ complex has a $Ru(3d_{5/2})$ photoelectron binding energy in the Ru(III) range.[36] The di-

(1) Current addresses: (a) Department of Chemistry, Mie University, Japan. (b) Department of Chemistry, Yangzhou Teacher's College, Jiangsu, People's Republic of China. (c) Department of Chemistry, Slovak Technical Institute, Bratislava, Czechoslovakia. (d) Central Research Laboratories, Kanegafuchi Chemical Industry Co. Ltd., Kobe 652, Japan.

(2) (a) McCleverty, J. A. *Prog. Inorg. Chem.* **1968**, *10*, 49. (b) Schrauzer, G. N. *Acc. Chem. Res.* **1969**, *2*, 72.

(3) Pierpont, C. G.; Buchanan, R. M. *Coord. Chem. Rev.* **1981**, *38*, 45.

(4) Haga, M.; Dodsworth, E. S.; Lever, A. B. P. *Inorg. Chem.* **1986**, *25*, 447.

(5) Boone, S. R.; Pierpont, C. G. *Inorg. Chem.* **1987**, *26*, 1769.

(6) Cass, M. E.; Gordon, N. R.; Pierpont, C. G. *Inorg. Chem.* **1986**, *25*, 3962.

(7) Lynch, M. W.; Buchanan, R. M.; Pierpont, C. G.; Hendrickson, D. N. *Inorg. Chem.* **1981**, *20*, 1038.

(8) Stallings, M. D.; Morrison, M. M.; Sawyer, D. T. *Inorg. Chem.* **1981**, *20*, 2655.

(9) Downs, H. H.; Buchanan, R. M.; Pierpont, C. G. *Inorg. Chem.* **1979**, *18*, 1736.

(10) Bodini, M. E.; Copia, G.; Robinson, R.; Sawyer, D. T. *Inorg. Chem.* **1983**, *22*, 126.

(11) Buchanan, R. M.; Claflin, J.; Pierpont, C. G. *Inorg. Chem.* **1983**, *22*, 2552.

(12) Kahn, O.; Prins, R.; Reedijk, J.; Thompson, J. S. *Inorg. Chem.* **1987**, *26*, 3557.

(13) Lynch, M. W.; Hendrickson, D. N.; Fitzgerald, B. J.; Pierpont, C. G. *J. Am. Chem. Soc.* **1984**, *106*, 2041.

(14) Sofen, S. R.; Ware, D. C.; Cooper, S. R.; Raymond, K. N. *Inorg. Chem.* **1979**, *18*, 234.

(15) Connelly, N. G.; Manners, I.; Protheroe, J. R. C.; Whiteley, M. W. *J. Chem. Soc., Dalton Trans.* **1984**, 2713.

(16) Lynch, M. W.; Valentine, M.; Hendrickson, D. N. *J. Am. Chem. Soc.* **1982**, *104*, 6982.

(17) Magers, K. D.; Smith, C. G.; Sawyer, D. T. *Inorg. Chem.* **1980**, *19*, 492.

(18) Griffith, W. P.; Pumphrey, C. A.; Rainey, T.-A. *J. Chem. Soc., Dalton Trans.* **1986**, 1125.

(19) Buchanan, R. M.; Kessel, S. L.; Downs, H. H.; Pierpont, C. G.; Hendrickson, D. N. *J. Am. Chem. Soc.* **1978**, *100*, 7894.

(20) Haga, M.; Dodsworth, E. S.; Lever, A. B. P.; Boone, S. R.; Pierpont, C. G. *J. Am. Chem. Soc.* **1986**, *108*, 7413.

(21) Jones, S. E.; Chin, D.-H.; Sawyer, D. T. *Inorg. Chem.* **1981**, *20*, 4257.

(22) Buchanan, R. M.; Fitzgerald, B. J.; Pierpont, C. G. *Inorg. Chem.* **1979**, *18*, 3439.

(23) Lynch, M. W.; Hendrickson, D. N.; Fitzgerald, B. J.; Pierpont, C. G. *J. Am. Chem. Soc.* **1981**, *103*, 3961.

(24) Larsen, S. K.; Pierpont, C. G.; DeMunno, G.; Dolcetti, G. *Inorg. Chem.* **1986**, *25*, 4828.

(25) Chin, D.-H.; Sawyer, D. T.; Schaefer, W. P.; Simmons, J. *Inorg. Chem.* **1983**, *22*, 752.

(26) Jones, S. E.; Leon, L. E.; Sawyer, D. T. *Inorg. Chem.* **1982**, *21*, 3692.

(27) deLearie, L. A.; Pierpont, C. G. *J. Am. Chem. Soc.* **1986**, *108*, 6393.

(28) Harmalker, S.; Jones, S. E.; Sawyer, D. T. *Inorg. Chem.* **1983**, *22*, 2790.

(29) Galeffi, B.; Postel, M. *Nouv. J. Chim.* **1984**, *8*, 481.

(30) Bristow, S.; Enemark, J. H.; Garner, C. D.; Minelli, M.; Morris, G. A.; Ortega, R. B. *Inorg. Chem.* **1985**, *24*, 4070.

(31) Wilshire, J. P.; Sawyer, D. T. *J. Am. Chem. Soc.* **1978**, *100*, 3972.

(32) Thompson, J. S.; Calabrese, J. C. *Inorg. Chem.* **1985**, *24*, 3167.

(33) Mulay, M. P.; Garge, P. L.; Padhye, S. B.; Haltiwanger, R. C.; deLearie, L. A.; Pierpont, C. G. *J. Chem. Soc. Chem. Commun.* **1987**, 581.

(34) Magnuson, R. H.; Taube, H. *J. Am. Chem. Soc.* **1975**, *97*, 5129.

(35) Creutz, C.; Chou, M. H. *Inorg. Chem.* **1987**, *26*, 2995.

0002-7863/88/1510-8076$01.50/0

oxolene data reported here provide additional insight into the electronic structures of such species.

Within a given redox series, the starting material as isolated from the initial synthesis is electrically neutral and is designated S. The symbols R1 and R2 refer to the first and second reduction products and O1 and O2 to the first and second oxidation products, respectively.

For clarity, the abbreviation (diox) will be used for a general ligand without definition of its oxidation state. The labels (DTBCat), (DTBSq), and (DTBQ), etc. are used to indicate catecholate(2−), semiquinone(radical 1−), and quinone(0) oxidation states where both substituent and oxidation state are defined. The labels cat, sq, and q are used for a species of defined oxidation state with indeterminate substituent. A label such as DTBDiox defines the substituent but not the oxidation state of the ligand.

Experimental Section

Methods. Electronic spectra were recorded with a Hitachi-Perkin Elmer microprocessor Model 340 spectrometer or a Guided Wave Inc. Model 100-20 optical waveguide spectrum analyser with a WP100 fiber optic probe. Electrochemical data were collected with a Pine Model RDE3 double potentiostat or with a Princeton Applied Research (PARC) Model 173 potentiostat or a PARC Model 174A polarographic analyser coupled to a PARC Model 175 universal programmer. Cyclic and differential pulse voltammetry were carried out with platinum wire working and counter electrodes and a silver wire quasi-reference electrode. Potentials were referenced internally to the ferricenium/ferrocene couple (Fc^+/Fc, 0.31 V versus SCE).[37] Spectroelectrochemical measurements utilized an optically transparent thin-layer electrode (OTTLE) cell with a gold minigrid working electrode (500 lines/in.)[38] or a bulk electrolysis cell consisting of a platinum plate working electrode, and a platinum flag counter electrode and a silver wire quasi-reference electrode separated from the working compartment by medium glass frits. The fiber optic probe was immersed in the solution to obtain electronic spectra of the products.

Electron spin resonance spectra were obtained with a Varian E4 spectrometer calibrated with diphenylpicrylhydrazide (DPPH). Where ESR spectra of electrochemically generated species were required, these were prepared under nitrogen inside a Vacuum Atmospheres Drilab and transferred to ESR tubes. Control electronic spectra were also recorded. NMR data were obtained with a Bruker AM300 FT NMR spectrometer. Magnetic data were obtained through the courtesy of Prof. L. K. Thompson (Memorial University, Newfoundland) with a Faraday balance. Photoelectron spectra (PES) were recorded at the Surface Science Centre in the University of Western Ontario, London, Ontario. Fourier transform infrared (FTIR) data were obtained with a Nicolet SX20 spectrometer, as KBr disks or as Nujol or hexachlorobutadiene mulls. Resonance Raman (rR) data were obtained through the courtesy of Prof. D. J. Stufkens, University of Amsterdam, with apparatus and conditions as described previously.[39] Microanalyses were carried out by Canadian Microanalytical Service Ltd., New Westminster, BC.

Materials. Tetrabutylammonium perchlorate (TBAP, Kodak) was recrystallized from absolute ethanol and dried in a vacuum oven at 50 °C for 2 days. 1,2-Dichlorobenzene (DCB, Aldrich Gold Label) and 1,2-dichloroethane (DCE, Aldrich Gold Label) were used as supplied. Dichloromethane and diethyl ether (Aldrich, Reagent Grade) were dried over molecular sieves and distilled under nitrogen prior to use. Ru(bpy)Cl_3 was prepared according to the literature.[40] Cobaltocene (Cp_2Co, Strem Chemical Company) was used as supplied. 3,5-Di-*tert*-butylcatechol (Aldrich) was purified by recrystallization from benzene. Catechol was purchased from Tokyo Kasei or Aldrich and was recrystallized twice from ethanol. 3,4,5,6-Tetrachlorocatechol was prepared by reduction of *o*-chloranil as follows. To a stirred solution of *o*-chloranil (2.0 g, 8.13 mmol) in glacial acetic acid (20 mL) was added dropwise a solution of $SnCl_2 \cdot 2H_2O$ (14 g, 62 mmol) in 12 M HCl (30 mL). The orange color of the solution first darkened and then faded as the product precipitated. After complete addition, the resulting mixture was stirred at ambient temperature for 30 min. The crude product was filtered, washed with 12 M HCl, and then dried in vacuo. Recrystallization from $EtOH/H_2O$ gave the monohydrate (88% yield): mp 182–184 °C, lit.[41] 194–195 °C.

Preparation of Complexes. All manipulations were carried out under nitrogen or argon, with standard Schlenk techniques, except where stated.

Ru(bpy)(DTBDiox)$_2$ (1,S). To degassed methanol (30 mL) were added Ru(bpy)Cl_3 (0.29 g, 0.80 mmol) and DTBCatH_2 (0.34 g, 1.5 mmol). The resultant slurry was refluxed for 20 min. Addition of a solution of NaOH (0.12 g, 3.04 mmol) in methanol (10 mL) then gave a deep blue solution which was refluxed for 24 h. After having been cooled to room temperature the mixture was exposed to air, and water (5 mL) was added. Upon cooling (−5 °C, 24 h) the product precipitated as a dark blue powder, which was recrystallized from methanol/water (87% yield). Samples for ESR were purified further by gel filtration on Sephadex LH20 with 1,2-dichloroethane as solvent: ^1H NMR data (in C_6D_6 with 20% $CDCl_3$, scale ppm downfield from TMS) 7.64–6.40 m, 1.68 s, 1.67 s, 1.34 s, 1.33 s, 1.31 (4) s, 1.31 (0) s, 1.26 s. Anal. Calcd for $C_{38}H_{48}N_2O_4Ru$: C, 65.4; H, 6.9; N, 4.0. Found: C, 65.2; H, 6.9; N, 4.0.

Ru(bpy)(Diox)$_2$ (2,S). This compound was prepared with catechol in a procedure analogous to that described above for **1,S**. After exposure of the reaction mixture to air, it was filtered immediately and allowed to stand at ambient temperature for 72 h. Deep blue crystals of the product were isolated by filtration and washed with methanol (45% yield). Samples for ESR were purified by gel filtration as above: ^1H NMR data (in $CDCl_3$, scale ppm downfield from TMS) 8.31 d (J = 8.03 Hz), 2 H, 7.91 td (J = 7.40, 1.66 Hz), 2 H, 7.43–7.36 m, 4 H, 7.32 dd (J = 8.16, 1.15 Hz), 2 H, 7.16 dd (J = 8.28, 1.35 Hz), 2 H, 6.94 td (J = 7.14, 1.58 Hz), 2 H, 6.84 td (J = 8.24, 1.58 Hz), 2 H. Anal. Calcd for $C_{22}H_{16}N_2O_4Ru$: C, 55.8; H, 3.4; N, 5.9. Found: C, 54.5; H, 3.4; N, 5.7. This compound was analyzed several times, and a better C analysis could not be obtained; it may be partially hydrated.

Ru(bpy)(TClDiox)$_2$ (3,S). This compound was prepared with tetrachlorocatechol in a procedure analogous to that described above for **1,S**. After exposure to air the reaction mixture was left at ambient temperature for 48 h. Filtration of this mixture gave a crude material which contained primarily a dark green byproduct. The desired product was extracted from this solid with several portions of boiling dichloromethane. The combined extracts were concentrated in vacuo, and methanol was then added to initiate crystallization. This mixture was stored at −5 °C for 72 h. Dark blue crystals of pure Ru(bpy)(TClDiox)$_2$ (5% yield) were filtered off and washed with cold methanol. Anal. Calcd for $C_{22}H_8Cl_8N_2O_4Ru$: C, 35.3; H, 1.1; N, 3.7. Found: C, 34.8; H, 1.1; N, 3.4.

[Ru(bpy)(DTBDiox)$_2$]ClO_4 (1,O1). To a stirred solution of Ru(bpy)(DTBDiox)$_2$ (69.9 mg, 0.098 mmol) in dichloromethane (3 mL) at 0 °C was added a solution of $AgClO_4$ (20 mg, 0.098 mmol) in acetonitrile (0.5 mL). Silver metal began to precipitate immediately, and the mixture became deep purple. After 15 min the mixture was filtered through a short plug of Celite (7 mm × 50 mm) to remove the metallic silver. The volume of the filtrate was reduced to 2 mL, and a mixture of diethyl ether and hexanes was added to initiate crystallization. The mixture was left at −5 °C for 24 h. After filtration, purple crystals of the product were obtained (91% yield). Anal. Calcd for $C_{38}H_{48}ClN_2O_8Ru$: C, 57.2; H, 6.1; N, 3.5. Found: C, 56.8; H, 6.1; N, 3.7. The hexafluorophosphate salt was prepared similarly, with $AgPF_6$ in place of $AgClO_4$; its spectra (IR and electronic) were in agreement with those of the perchlorate.

[Cp_2Co][Ru(bpy)(Diox)$_2$] (2,R1). Cobaltocene (50.2 mg, 0.27 mmol) was added to a solution of Ru(bpy)(Diox)$_2$ (0.112 g, 0.24 mmol) in dichloromethane (30 mL) in an oxygen-free environment (drybox). The resulting dark green solution was stirred for 2 h and then filtered under pressure in the drybox. The dark green microcrystalline product (84% yield) was washed with diethyl ether and dried in vacuo. Anal. Calcd for $C_{32}H_{26}CoN_2O_4Ru$: C, 58.0; H, 4.0; N, 4.2. Found: C, 54.8; H, 3.9; N, 4.1. Some difficulty was experienced in obtaining a better C analysis for this product; its electronic spectrum is in agreement with the spectroelectrochemical data.

Results

Two series of compounds were prepared; one is based on Ru(bpy)(diox)$_2$, necessarily with a cis configuration, and the other is a series of *cis*- and *trans*-Ru(R-py)$_2$(diox)$_2$, to be described elsewhere,[42] but whose comparative electronic properties are

(36) Shepherd, R. E.; Proctor, A.; Henderson, W. W.; Myser, T. K. *Inorg. Chem.* **1987**, *26*, 2440.
(37) (a) Mann, C. K.; Barnes, K. K. "Electrochemical Reactions in Nonaqueous systems", Marcel Dekker, New York, 1970. (b) Gritzner, G.; Kuta, J. *Electrochim. Acta* **1984**, *29*, 869.
(38) Nevin, W. A.; Lever, A. B. P. *Anal. Chem.* **1988**, *60*, 727.
(39) Stufkens, D. J.; Snoeck, Th. L.; Lever, A. B. P. *Inorg. Chem.* **1988**, *27*, 953.
(40) (a) Krause, R. A. *Inorg. Chim. Acta* **1977**, *22*, 209. (b) Anderson, S.; Seddon, K. R. *J. Chem. Res.* **1979**, 74.
(41) Handbook of Chemistry and Physics, 54th Edition, Ed. R. C. Weast, 1973–74, CRC Press.
(42) Lever, A. B. P.; Auburn, P. R.; Dodsworth, E. S.; Haga, M.; Liu, W.; Nevin, W. A., to be submitted for publication.

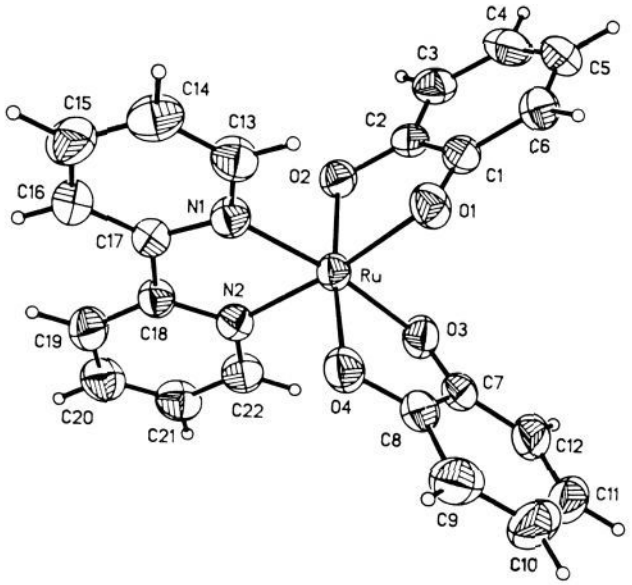

Figure 1. Molecular structure of $Ru(bpy)(Diox)_2$ (**2,S**).[43]

Table I. A Selection of Important Bond Distances and Angles for $Ru(bpy)(Diox)_2$ (**2,S**)[a]

bond distances (Å)		bond angles (deg)	
Ru–O(1)	2.003 (4)	O(1)–Ru–O(2)	81.8 (1)
Ru–O(2)	1.977 (3)	O(2)–Ru–O(3)	94.9 (1)
Ru–O(3)	1.995 (3)	O(1)–Ru–O(3)	88.0 (1)
Ru–O(4)	1.981 (3)	O(1)–Ru–O(4)	91.9 (1)
Ru–N(1)	2.042 (3)	O(2)–Ru–O(4)	173.1 (1)
Ru–N(2)	2.055 (4)	O(3)–Ru–O(4)	82.0 (1)
O(1)–C(1)	1.316 (5)	O(1)–Ru–N(2)	173.2 (1)
O(2)–C(2)	1.326 (6)	O(3)–Ru–N(1)	172.0 (2)
O(3)–C(7)	1.322 (4)	N(1)–Ru–N(2)	78.2 (2)
O(4)–C(8)	1.321 (5)		
C(1)–C(2)	1.424 (6)		
C(7)–C(8)	1.413 (6)		

[a] $R = 0.042$, $R_w = 0.053$ for 2853 reflections. See Figure 1 for numbering scheme. See ref 5 and 20 for X-ray data for $Ru(4\text{-}t\text{-}Bupy)_2(DTBDiox)_2$.

Table II. Electrochemical Data for $Ru(bpy)(diox)_2$ in 1,2-Dichloroethane, $E_{1/2}$ versus SCE[a]

diox	I	II	III	IV	V
DTBDiox	+1.55 ir	+0.89	+0.20	−0.82	−1.53 qr
Diox	+1.40 ir	+1.01 qr	+0.37	−0.53	−1.35
TClDiox	+1.54 ir	+1.25 ir	+0.88	−0.00	−0.95

[a] Data recorded against the ferricenium/ferrocene couple as internal calibrant and corrected to SCE by assuming the Fc^+/Fc couple lies at +0.31 versus SCE.[37] ir = irreversible; qr = quasi-reversible. The bulk solution is the starting material species ($1–5 \times 10^{-4}$ M) with 0.1–0.2 M TBAP as supporting electrolyte. The couples are reversible unless otherwise stated. $E_{1/2}$ values obtained by cyclic and differential pulse voltammetry are essentially identical.

relevant to the discussion of the bpy series. The materials obtained from the reaction mixture, $Ru(bpy)(diox)_2$, the so-called starting materials (labeled S), possess no counter ions and are air-stable, dark blue crystalline compounds. Single-crystal X-ray data are available for the $Ru(bpy)(Diox)_2$ (**2,S**) species (Figure 1)[43] and for the related *trans*-$Ru(4\text{-t-Bupy})_2(DTBDiox)_2$ (**4t,S**) compound.[5,20] Relevant bond distances are shown in Table I. One example each of an oxidized and reduced complex was isolated in the solid state.

(i) Electrochemistry. Table II contains electrochemical data for the starting materials, generally showing five one-electron redox

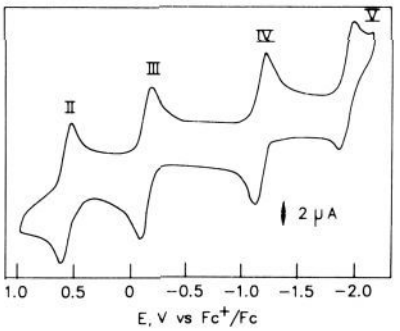

Figure 2. Cyclic voltammogram of 5.6×10^{-4} M $[Ru(bpy)(DTBDiox)_2]ClO_4$ (**1,O1**) in DCE solution with 0.1 M TBAP. Scan speed = 200 mV s^{-1}.

Table III. Electron Spin Resonance Data

	complex	g factors	peak to peak (G)	conditions
1,R1	$[Ru(bpy)(DTBDiox)_2]^-$[a]	2.076	92	DCE/rt[c]
		$1.937(_\parallel)$	35	DCB/77 K
		$2.100(_\perp)$		
2,R1	$Cp_2Co[Ru(bpy)(Diox)_2]$	$1.934(_\parallel)$	200	solid/77 K
		$2.109(_\perp)$[b]		
1,O1	$[Ru(bpy)(DTBDiox)_2]^+$[a]	1.964	210	DCE/rt[c]
		1.985	48	CH_2Cl_2/77 K
1,O1	$[Ru(bpy)(DTBDiox)_2]ClO_4$	$1.984(_\perp)$	42	solid/77 K
		$2.023(_\parallel)$		

[a] Electrochemically generated via bulk electrolysis. [b] Rhombic distortion. [c] Room temperature is abbreviated as rt.

processes (Figure 2), near +1.4–1.5 (I), +0.9–1.2 (II), +0.2–0.9 (III), 0–(−0.8) (IV), and −0.9–(−1.5) (V) V versus SCE. The bulk solution rest potentials for the starting materials lie between redox couples (III) and (IV). Couples (II)–(V) are usually reversible (but see Table II for details) showing $i_c/i_a = 1$, $i \propto v^{1/2}$, and peak-to-peak separations in the cyclic voltammogram (for reversible species) approaching 60 mV at slow scan rates (20 mV s^{-1}). The oxidation process (I) is invariably irreversible. The oxidized species $[Ru(bpy)(DTBDiox)_2]ClO_4$ (**2,01**), in bulk solution, gives similar voltammetry (the same redox couple potentials) to the starting material in DCE but has a different rest potential. The reversibility of most of the couples is an indication that structural changes such as dimerization or ligand loss are not taking place on the time scale of the experiment.

(ii) Nuclear Magnetic Resonance Spectra. The starting materials all give sharp and unshifted NMR spectra, implying the absence of paramagnetic species in the solutions.[44–46] For the (necessarily cis) $Ru(bpy)(DTBDiox)_2$ (**1,S**) there are three possible structural isomers depending upon the relative positions of the *tert*-butyl groups on the two dioxolene ligands. These three isomers give rise to eight possible *tert*-butyl resonances. In fact seven may be observed with 20% $CDCl_3$ in C_6D_6 solvent mixture, showing that all three isomers are present in solution and that there is an accidental degeneracy of two resonances.

(iii) Magnetic Susceptibility Measurements. The O1 species $[Ru(bpy)(DTBDiox)_2]ClO_4$ (**1,O1**) has one unpaired electron/molecule and a Curie–Weiss dependence of the magnetic susceptibility ($\chi_M = 0.329/(T + 4.78)$, $R = 0.999$, 32 points). The room temperature (295 K) moment is 1.63 μ_B, declining gradually to 1.51 μ_B at 5 K.

Although their solutions appear diamagnetic from the NMR data, the solid starting materials, S, have moments of the order of 1 μ_B/molecule or less at room temperature, consistent with temperature independent paramagnetism.

(iv) Electron Spin Resonance Spectra. The starting materials, **1,S** and **2,S**, are ESR-silent at room temperature (solid or solution)

(43) Boone, S. R.; Pierpont, C. G., to be submitted for publication.

(44) Buchanan, R. N.; Pierpont, C. G. *J. Am. Chem. Soc.* **1980**, *102*, 4951.
(45) Ref. 23 cited in ref. 5.
(46) Pell, S. D.; Salmonsen, R. B.; Abelleira, A.; Clarke, M. J. *Inorg. Chem.* **1984**, *23*, 385.

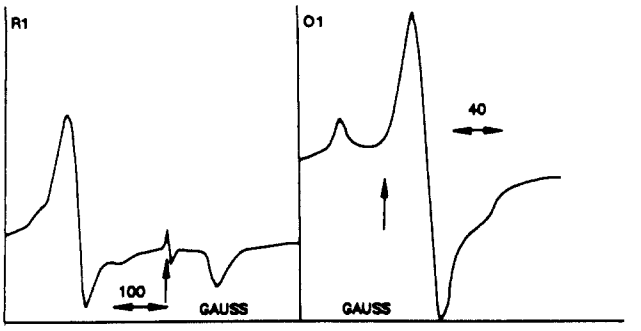

Figure 3. ESR spectra of (left) $[Ru(bpy)(DTBDiox)_2]^-$, (**1,R1**), 1.4×10^{-3} M in DCB at 77 K, and (right) $[Ru(bpy)(DTBDiox)_2]^+$, (**1,O1**), in the solid state at 77 K. The arrows denote the positions of the DPPH signals.

Table IV. Fourier Transform Infrared Spectra—Principal Absorption Bands

	complex	conditions	principal bands[a] (cm^{-1})
2,R1	$Cp_2Co[Ru(bpy)(Diox)_2]$	KBr	735, 768, *1253*, 1385, *1415*, 1464, 1559
1,S	$Ru(bpy)(DTBDiox)_2$	KBr	505, 773, 1024, 1099, *1142*, 1360, 1375, 1464, 1518, 1583
2,S	$Ru(bpy)(Diox)_2$	KBr	527, 728, 743, 772, *1099*, *1113*, *1208*, 1315, *1415*, 1448, 1532
3,S	$Ru(bpy)(TClDiox)_2$	KBr	767, 798, 979, *1188*, 1322, 1384, 1396, 1421
1,O1	$[Ru(bpy)(DTBDiox)_2]ClO_4$	Nujol	728, 773, 987, 1027, 1091,[b] 1238, 1339, 1361,[c] 1448,[c] 1466,[c] 1582

[a] Only the more prominent peaks are recorded here. Where one or more peaks clearly dominate the spectrum, they are in italics. [b] Hexafluorophosphate salt. [c] Hexachlorobutadiene mull. Perchlorate absorption, where present, is not reported.

and at 77 K in frozen DCE. In the solid state at 77 K very weak signals can be detected at $g = 2$; these are believed to be due to trace amounts of a free-radical impurity since stronger signals are observed in samples which have not been purified by gel filtration. R1 and O1 species yield rather broad signals very close to $g = 2$ in solution at room temperature, but at 77 K in the solid state, or in frozen DCB solution, sharp, free radical-like, axial or slightly rhombic signals are observed (Figure 3, Table III). For the oxidized species, O1, $g_\parallel > g_\perp$, while the reverse is true for the reduced species; the difference between $g_\parallel$ and $g_\perp$ is ~0.2 for R1 and ~0.04 for O1.

The electrochemically generated R2 species are ESR-silent at room temperature and at 77 K. Solutions of O2 are unstable.

(v) **Fourier Transform Infrared Spectra.** The principal FTIR absorption bands are given in Table IV. None of the starting materials show features typical of either catechol or semiquinone coordination. The spectra of all the S species (including the *cis*- and *trans*-R-py analogues)[42] are dominated by a strong absorption

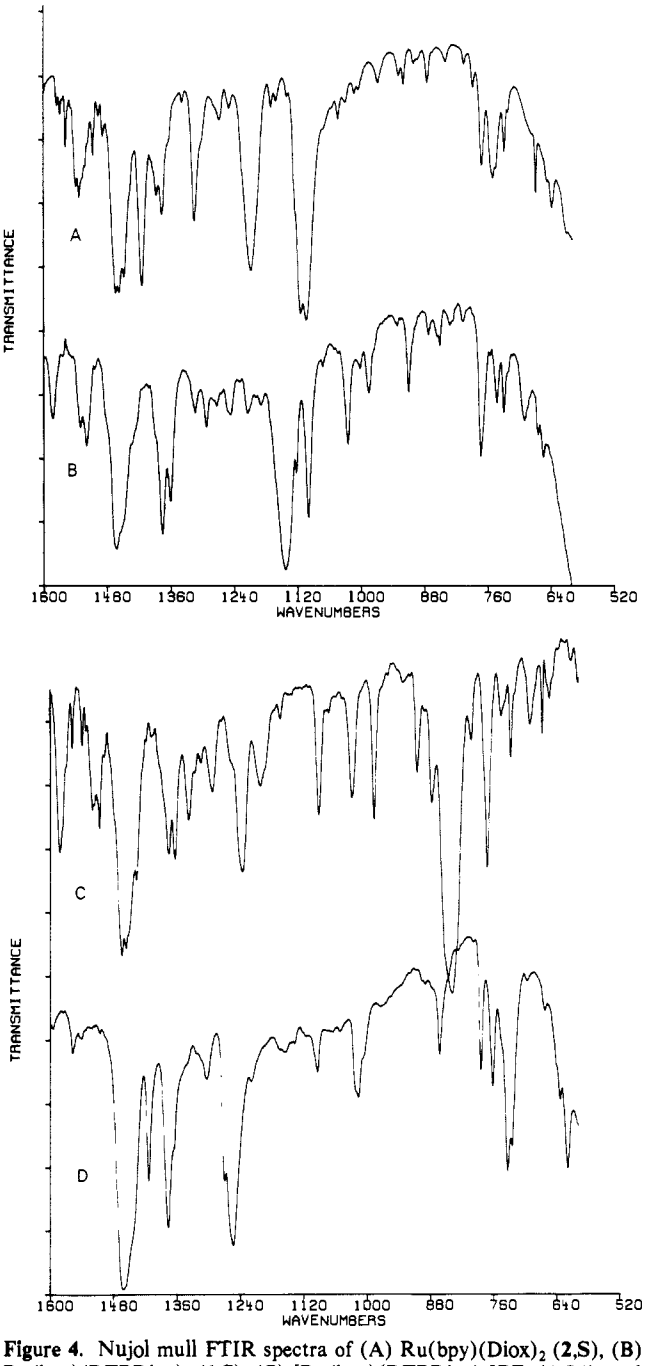

Figure 4. Nujol mull FTIR spectra of (A) $Ru(bpy)(Diox)_2$ (**2,S**), (B) $Ru(bpy)(DTBDiox)_2$ (**1,S**), (C) $[Ru(bpy)(DTBDiox)_2]PF_6$ (**1,O1**), and (D) $[Cp_2Co][Ru(bpy)(Diox)_2]$ (**2,R1**).

in the region 1100–1200 cm^{-1} (Figure 4A,B). The FTIR spectrum of a reduced complex (Figure 4D) is consistent with the

Table V. Photoelectron Emission Data

	complex	binding energy[a,b] (eV)		
		$Ru(3d_{5/2})$	O (1s)	N (1s)
2,R1	$[Cp_2Co][Ru(bpy)(Diox)_2]$	280.4	*c*	399.6
1,S	$Ru(bpy)(DTBDiox)_2$	280.8	530.7 (0.45)	399.7 (0.71)
			532.0 (0.33)	400.6 (0.29)
			533.0 (0.21)	
2,S	$Ru(bpy)(Diox)_2$	281.3	531.8 (0.52)	399.9
			532.4 (0.31)	
			533.8 (0.19)	
1,O1	$[Ru(bpy)(DTBDiox)_2]ClO_4$[d]	282.0	*c*	400.5
5,S	$[Ru(bpy)_2(DTBSq)]PF_6$	280.8[e]	531.4	399.6 (0.44)
				400.9 (0.56)

[a] Binding energies are given relative to C(1s) at 285.0 eV. Maximum error is ±0.3 eV. [b] Relative intensities in parentheses. [c] Contamination with silicone grease. [d] Perchlorate ion Cl(2p) observed at 207.5 (0.64) and 209.1 (0.36). [e] Additional signal observed at 281.8 eV believed to be due to differential charging problems. This complex reported in ref 4.

Table VI. Electronic Spectroscopic Data for Ru(bpy)(diox)$_2$ Redox Series in 1,2-Dichlorobenzene; λ_{max} (nm) (ϵ(L mol^{-1} cm^{-1}))[a]

species	color	DTBDiox (1)	Diox (2)	TClDiox (3)
R2	red-brown	865 (2950)		
		740 (3150)		750 br (3500)
		570 sh[c]		505 sh
		490 (8150)		470 (8700)
		330 sh		
R1	green	850 (6600)	ca. 780 sh	760 sh
		695 (9200)	680	620 (ca. 7000)
		430 (5150)	400 sh	400 (ca. 5000)
S	deep blue	1175 (6050)	1235 (4400)	1315 (4290)
		955 (12100)	955 (14400)	1005 (16100)
		605 (11600)	590 (11100)	585 (10040)
		505 (3100) sh	475 (3600)	450 sh
		375 (5700)	340	420 (4140)
O1	violet	720 (11100)	720	800 (ca. 9700)
		505 (6550)	515	560 (ca. 7100)
		390 (5700)	390 sh	385 sh
O2	brown-yellow	950 (770)		*b*
		570 (3150)		
		390 (3220)		

[a] Solutions of oxidized and reduced species prepared by controlled potential electrolysis and, in the cases of **1,O1**, **1,R1**, and **2,R1**, also by chemical oxidation or reduction. [b] Solution unstable. [c] sh = shoulder.

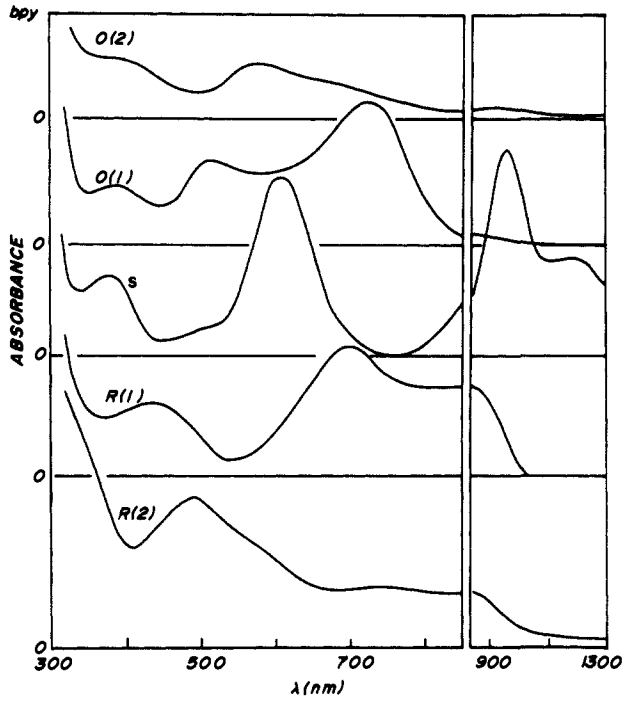

Figure 5. Electronic spectra of the redox series based on Ru(bpy)-(DTBDiox)$_2$, in DCB solution, prepared by controlled potential electrolysis. The labeling system is explained in the text.

presence of a catecholate moiety, but that of an oxidized species (Figure 4C) does not provide clear evidence of oxidation state.

(vi) Photoelectron Spectra. Data for the Ru($3d_{5/2}$) and core levels of oxygen and nitrogen are shown in Table V. The lowest Ru($3d_{5/2}$) binding energy occurs in R1 and the highest in O1. The N(1s) and O(1s) energies follow roughly the same trend but with smaller differences.

(vii) Electronic Spectra. Table VI contains electronic spectroscopic data for the starting materials and a selection of their oxidation and reduction products. Clean reactions with isosbestic points were generally observed in these redox processes. The electronic spectra of O2, O1, S, R1, and R2 are shown for the **1** redox series in Figure 5. In general, all members of a given oxidation *label*, i.e., O1, R1, etc., have very similar shaped spectra. Many of the absorption bands show significant dependence upon the dioxolene substituent. Spectra of representative complexes in the solid state (in Nujol mulls) are similar to the corresponding solution spectra. The S series is remarkable in the very intense near-IR absorption, absent from all other oxidation states, but

Table VII. Resonance Raman Spectra[a]

species	excitation wavelength (nm)	enhanced frequencies (cm^{-1})
1,S	488	*1600*, 1550, *1480*, 1165, 990, 590, 575, 450
	570	1550, *1475*, *1320*, 1165, 690, *590* vs, *575* vs, 535, 505, 490, *450* vs, 395, 220, *195*, 155
3,S	457.9	1600, 1550, 1485, *565*
	580	1520, 1485, 1375, 1125, 810, *615*, *565* vs, 540, *490*, 370, 360, 340, 320, 230, 140
1,O1	488 or 514	1495, 1407, 1362, 935, 915, *591*, *564* vs, *524*
	620	1407, 935, 915, 591, *564* vs, *524*

[a] Spectra were run in 1,2-dichloroethane. Strong bands are in italics and the most strongly enhanced are marked vs.

Chart I

R2	(a)	$[Ru^{II}(bpy)(cat)_2]^{2-}$
	(b)	$[Ru^{III}(bpy^-)(cat)_2]^{2-}$
R1	(a)	$[Ru^{II}(bpy)(cat)(sq)]^-$
	(b)	$[Ru^{III}(bpy)(cat)_2]^-$
S	(a)	$Ru^{II}(bpy)(sq)_2$
	(b)	$Ru^{III}(bpy)(cat)(sq)$
	(c)	$Ru^{IV}(bpy)(cat)_2$
O1	(a)	$[Ru^{II}(bpy)(sq)(q)]^+$
	(b)	$[Ru^{III}(bpy)(sq)_2]^+$
	(c)	$[Ru^{IV}(bpy)(cat)(sq)]^+$
O2	(a)	$[Ru^{II}(bpy)(q)_2]^{2+}$
	(b)	$[Ru^{III}(bpy)(sq)(q)]^{2+}$

present in the monosemiquinone ruthenium species.[4] Resonance Raman spectra of three compounds were obtained in order to clarify the assignments of the spectra (see Table VII). Full details of these will appear elsewhere.[47]

Discussion

In the previous dioxolene literature, mixed-valence compounds have generally been interpreted in terms of localized structures.[11,16,44] Moreover, in Co(bpy)(DTBSq)(DTBCat) and Mn-(py)$_2$(DTBSq)$_2$ discontinuous changes in formal oxidation state have been observed with change of temperature.[13,23,44] Nevertheless, ESR studies of many dioxolene complexes have shown that delocalization occurs to a small extent,[6,9,48] and in one recent case this has been supported by extended Hückel and fragment molecular orbital calculations.[48] However, it has been thought previously that extensive delocalization did not occur in dioxolene complexes and that oxidation states could be unambiguously

(47) Stufkens, D. J.; Lever, A. B. P., to be submitted for publication.
(48) Bianchini, C.; Masi, D.; Mealli, C.; Meli, A.; Martini, G.; Laschi, F.; Zanello, P. *Inorg. Chem.* **1987**, *26*, 3683.

defined.[3] Ruthenium dioxolenes are the first dioxolene complexes in which significant delocalization has been demonstrated.[4,5]

By using the normal oxidation state conventions, with localization of electrons, these species could exist as a number of possible electronic isomers. The most reasonable possibilities are shown in Chart I. We consider first the oxidation state information which may be derived from the various techniques.

All the redox potentials depend significantly upon the substituents in the dioxolene ring. Upon replacement of DTBCat by TClCat the potentials shift 0.36, 0.68, 0.82, and 0.58 V for couples (II)–(V), respectively. Similar dependencies are seen in the corresponding *trans*-4-*tert*-butylpyridine data set,[42] except for couple (V) whose dependence essentially disappears. A large dependence may imply a redox process which is localized on the dioxolene ligands, while a small or zero dependence indicates a redox process on the metal ion.[49] In the $Ru(bpy)_2$(diox) and $Ru(py)_4$(diox) series, the shifts in both redox processes involving the dioxolene ligands were about 0.5 V when TClDiox replaced DTBDiox.[4] Differences of about 0.7 V are observed for both the free ligands reductions (q/sq and sq/cat) when comparing TClDiox and DTBDiox,[8] and larger differences (0.7–1.2 V) occur in the complexes[11] Cr^{III}(bpy)(sq)(cat) and[9] $[Cr^{III}(cat)_3]^{3-}$.

With regard to ESR spectra, we are concerned with distinguishing a Ru(III) center from a Ru(II) center bound to a free radical. Low spin Ru(III) $(t_{2g})^5$ species exhibit ESR spectra which are usually highly anisotropic with axial or rhombic symmetry.[50] For example, $[Ru^{III}(NH_3)_4(cat)]^+$ cations give axial spectra with $g_\parallel = \sim 1.9$ and $g_\perp = \sim 2.7$.[46] On the other hand a radical bound to Ru(II) will exhibit a narrow signal close to $g = 2$. Nevertheless, in certain reduced $[Ru(bpy)_3]^{(2-n)+}$ species, ligand-localized electrons show slightly anisotropic signals with $g_\parallel < g_\perp$ and difference of up to ~0.04 between the g values.[51] Ruthenium phosphine semiquinone complexes,[52,53] also with $g_\parallel < g_\perp$, have similar anisotropy ($g_\parallel = 2.00$, $g_\perp = 2.02$). The $[Ru(bpy)_2$(DTBSq)$]^+$ cation[4] shows slight anisotropy, $g_\parallel > g_\perp$, similar to the O1 species.

The IR spectra of dioxolene complexes can normally be used without ambiguity to define the oxidation state of the dioxolene ligand.[16,46,54-56] The C–O frequency is particularly characteristic and gives rise to relatively intense absorption at[16-19,46,54-57]

coordinated quinones	C=O	1600–1675 cm^{-1}
semiquinones	C---O	1400–1500
catechols	C—O	1250, 1480 (ring breathing)

The strong band observed near 1150 cm^{-1} in the S series complexes has almost no precedent in the literature. Strong bands in this region have been reported in only one other case, a series of four-coordinate copper(II) complexes of DTBSq with nitrogen-donor coligands.[32] These complexes show one or two strong bands between 1110 and 1160 cm^{-1}, which were not assigned, and there are no strong features in the 1450 cm^{-1} region where typical semiquinone absorptions occur.

With PES, inner shell binding energies of metals in complexes may be used (with caution) to infer the oxidation state of the metal.[58a] Typically, the binding energy increases by about 1 eV per unit increase in oxidation state regardless of the charge on the metal.[58b] There are exceptions, however, particularly where π-bonding ligands are present. Comparisons are best made within a series of complexes having similar ligands. The $3d_{5/2}$ binding energies for Ru(II) and Ru(III) normally lie in the ranges 280–282 and 282–283 eV, respectively,[36,58] though a binuclear species formally containing both Ru(III) and Ru(IV) shows only one peak at 282.9 eV,[58e] and an (*N*-methylpyrazinium)ruthenium pentaammine complex which formally contains Ru(II) has a binding energy of 282.2 eV, in the Ru(III) range.[36] The nitrogen 1s binding energy is known to be sensitive[59] to variation in charge on the atom to which it is bound. However, the variation in N(1s) energies in this series of complexes is too small to draw any conclusions.

Following the discussion of electronic spectra presented previously,[4] one may observe metal-to-ligand charge transfer (MLCT) from Ru(dπ) to acceptor orbitals on bpy, sq, or q and/or ligand-to-metal charge transfer (LMCT) from cat, sq or bpy to Ru(III), internal semiquinone, and interligand charge transfer (ILCT) transitions, all of which might occur in the visible region. The charge-transfer transitions will have energies depending on the oxidation state of ruthenium and the dioxolene ligand and should depend in a predictable manner on the dioxolene substituents. The weaker ligand field transitions are likely to be obscured in these systems.

Catecholate derivatives of difficult to reduce metal ions show no visible absorption other than d–d,[28,53,60,61] e.g., $[M(II)(cat)_2]^{2-}$ (M = Co, Ni, Cu). However, catecholate complexes of a reducible metal should show LMCT transitions. For example, complexes of iron(III), cerium(IV), and higher oxidation states of molybdenum and manganese show moderately intense (2000–5000 L mol^{-1} cm^{-1}) visible region transitions attributable to LMCT.[21,25,61-67] These might also be observed, shifted to the blue, in a semiquinone bound to a reducible metal ion.

The internal transition observed in the visible region in free semiquinones may also be observed as a weak absorption (ϵ ca. 800–5000 L mol^{-1} cm^{-1}) in semiquinone metal complexes, shifted a little from its free ligand position; e.g., $DTBSq^-$ 690 nm (800), $Zn^{II}(DTBSq)^+$ 740 nm (900),[10] [Co(trien)(DTBSq)]$^{2+}$ 512 nm (1200),[68] and $M^{II}(DTBSq)_2$(bpy) (M = Mn, Co, Ni) ca. 770 nm (2700).[13,44] A band similar in energy and intensity (ca. 700 nm (2500)) is seen[11] in $[Cr^{III}(DTBSq)_2(bpy)]^+$, but in this case there is also a more intense transition near 500 nm (7400). A similar transition (similar band envelope), with a molar absorption coefficient of almost 20 000 L mol^{-1} cm^{-1}, is observed in Cr^{III}-$(DTBSq)_3$.[11,14] It is unlikely that Cr(III) would exhibit such a low-energy LMCT transition, particularly as there is no such band in[14] $[Cr(DTBCat)_3]^{3-}$, so this transition probably also involves only the semiquinone ligands.

Complexes containing both a sq and a cat residue sometimes exhibit a broad, relatively weak (ca. 3000 L mol^{-1} cm^{-1}) transition in the red or near infrared (NIR) region which has been attributed

(49) Vlcek, A. A. *Electrochim. Acta* **1968**, *13*, 1063.
(50) (a) DeSimone, R. E. *J. Am. Chem. Soc.* **1973**, *95*, 6238. (b) Sakaki, S.; Hagiwara, N.; Yanase, Y.; Ohyoshi, A. *J. Phys. Chem.* **1978**, *82*, 1917. (c) Raynor, J. B.; Jeliazkowa, B. G. *J. Chem. Soc., Dalton Trans.* **1982**, 1185. (d) Hudson, A.; Kennedy, M. J. *J. Chem. Soc. A* **1969**, 1116. (e) Lahiri, G. K.; Bhattacharya, S.; Ghosh, B. K.; Chakravorty, A. *Inorg. Chem.* **1987**, *26*, 4324.
(51) (a) Motten, A. G.; Hanck, K. W.; DeArmond, M. K. *Chem. Phys. Lett.* **1981**, *79*, 541. (b) Morris, D. E.; Hanck, K. W.; DeArmond, M. K. *J. Am. Chem. Soc.* **1983**, *105*, 3032.
(52) Balch, A. L. *J. Am. Chem. Soc.* **1973**, *95*, 2723.
(53) Girgis, A. Y.; Sohn, Y. S.; Balch, A. L. *Inorg. Chem.* **1975**, *14*, 2327.
(54) Brown, D. G.; Johnson, W. L. *Z. Naturforsch.* **1979**, *34B*, 712.
(55) Wicklund, P. A.; Brown, D. G. *Inorg. Chem.* **1976**, *15*, 396.
(56) Brown, D. G.; Reinprecht, J. T.; Vogel, G. C. *Inorg. Nucl. Chem. Lett.* **1976**, *12*, 399.
(57) Wilson, H. W. *Spectrochim. Acta* **1974**, *30A*, 2141.
(58) (a) Srivastava, S. *App. Spec. Rev.* **1986**, *22*, 401. (b) Feltham, R. D.; Brant, P. *J. Am. Chem. Soc.* **1982**, *104*, 641. (c) Brant, P.; Stephenson, T. A. *Inorg. Chem.* **1987**, *26*, 22. (d) Connor, J. A.; Meyer, T. J.; Sullivan, B. P. *Inorg. Chem.* **1979**, *18*, 1388. (e) Weaver, T. R.; Meyer, T. J.; Adeyemi, S. A.; Brown, G. M.; Eckberg, R. P.; Hatfield, W. P.; Johnson, E. C.; Murray, R. W.; Untereker, D. *J. Am. Chem. Soc.* **1975**, *97*, 3039.
(59) Perry, W. B.; Schaaf, T. F.; Jolly, W. L. *J. Am. Chem. Soc.* **1975**, *97*, 4899.
(60) Isied, S. S.; Kuo, G.; Raymond, K. N. *J. Am. Chem. Soc.* **1976**, *98*, 1763.
(61) Rohrscheid, F.; Balch, A. L.; Holm, R. H. *Inorg. Chem.* **1966**, *5*, 1542.
(62) Espinet, P.; Bailey, P. M.; Maitlis, P. M. *J. Chem. Soc., Dalton, Trans.* **1979**, 1542.
(63) Sofen, S. R.; Cooper, S. R.; Raymond, K. N. *Inorg. Chem.* **1979**, *18*, 1611.
(64) Charney, L. M.; Finklea, H. O.; Schultz, F. A. *Inorg. Chem.* **1982**, *21*, 549.
(65) Anderson, B. F.; Buckingham, D. A.; Robertson, G. B.; Webb, J.; Murray, K. S.; Clark, P. E. *Nature (London)* **1976**, 722.
(66) Wilshire, J. P.; Leon, L.; Bosserman, P.; Sawyer, D. T. *J. Am. Chem. Soc.* **1979**, *101*, 3379.
(67) Hartman, J. R.; Foxman, B. M.; Cooper, S. R. *Inorg. Chem.* **1984**, *23*, 1381.
(68) Wicklund, P. A.; Beckman, L. S.; Brown, D. G. *Inorg. Chem.* **1976**, *15*, 1996.

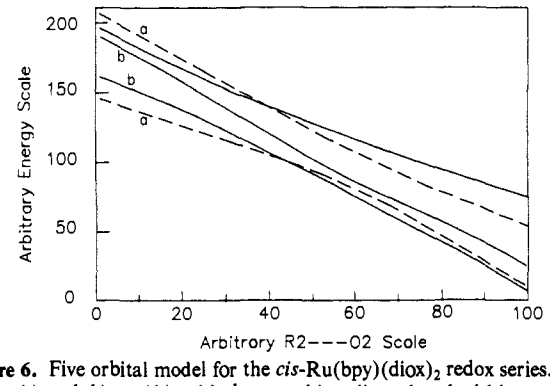

Figure 6. Five orbital model for the *cis*-Ru(bpy)(diox)$_2$ redox series. The L(a + b) and d(a + 2b) orbitals are arbitrarily ordered within each set. The left hand side of the diagram refers to R2 where E(L) < E(d). Moving across the diagram covers the range R1, S, O1, and O2 with E(L) > E(d) for O2. The essential features of this qualitative diagram are the crossing of the mainly L and d orbitals, the extensive mixing thereof, and the mainly d nature of the LUMO in R1 compared with mainly ligand in O1 and O2.

to an intervalence (interligand) transition.[16,44]

Five Orbital Model. The electronic structure, spectra, magnetism, and ESR of these species can be understood by using a simple, qualitative MO model constructed from the three 4d (t_{2g} in O_h) ruthenium orbitals and the frontier π ($3b_1$ in C_{2v} using the Gordon and Fenske nomenclature[69]) orbitals of the dioxolene ligands. We refer to this below as the five orbital model. From electrochemical data, it is evident that the bipyridine LUMO π_1^* is sufficiently high in energy,[70] and the dioxolene oxygen lone pairs (a_1 + b_2, in dioxolene plane) are sufficiently low (and have little overlap) that they are not considered to play a major role in influencing the oxidation states of metal and ligands. They are, however, relevant to the electronic spectra.

In the (maximum) C_2 symmetry of these species, the two ligand $\pi(3b_1)$ orbitals combine to yield (a + b), and the three d orbitals transform as (a + 2b). One ligand combination will couple to two d orbitals and the other to only one, resulting in a pronounced splitting of these ligand combinations. The three d orbitals all possess some ligand character (and vice versa) depending upon orbital overlap and the relative d and L orbital energies. These five MOs are filled with ten electrons in R2.

All five orbitals will become more stable going from R2 to O2, but those which are primarily metal in character will be stabilized more upon oxidation of the complex than those which are primarily ligand,[4,69,70] because of the greater spatial extent of the ligand orbitals. From the data discussed below, oxidation of R2 involves oxidation of Ru(II), at least to some degree; thus the ruthenium d(a,2b) orbitals lie at comparable or slightly higher energies than the catechol (a,b) combinations in R2. To be consistent with all the experimental data proceeding from R2 to O2 there must then be a crossover of these orbitals such that at O2 the ruthenium d(a,2b) orbitals lie below the ligand combinations (see Figure 6).

In the crossover region there will be extensive mixing of the d(a,2b) and L(a,b) orbitals. Placing nine, eight, and seven electrons into these five mixed orbitals, from R1 to O1, yields, from experiment, one, zero, and one unpaired electrons, respectively and leaves the uppermost level of the five half-full in R1 and empty in S and O1. This approach is validated in the *trans*-Ru(R-py)$_2$(diox)$_2$ series[42] where two of the three d orbitals are unmixed because of the higher symmetry (D_{2h}). It is evident that one of these d orbitals is uppermost in the [Ru(3-Clpy)$_2$(DTBCat)$_2$]$^-$ R1 species which is exclusively Ru(III), as indicated by its typical rhombic ESR spectrum.[42]

The effective oxidation state of the metal is determined by the total number of electrons in each MO scaled by the d orbital contribution to that MO. Similarly the average effective oxidation state of the pair of dioxolene ligands is determined by the total scaled occupancy of all orbitals having a contribution from the dioxolene ligands. Since the uppermost (of the five) orbital in R1 contains one unpaired electron, and this orbital is mixed Ru(d) and L, then an electron count must lead to the conclusion that the central ion in R1 is between Ru(II) and Ru(III), shifting to the latter as this orbital approaches a pure Ru(d) orbital. Similar arguments can be applied to the other members of the redox series. On passing from R1 to O2 the upper orbitals will contain an increasing proportion of L(a,b) so that the more oxidized species will approximate more closely to ruthenium(II).

By using the five orbital model, the structural and electronic identification of the various members of the redox series can be approached. Since this qualitative model does not indicate the ordering within the group of metal or ligand orbitals per se, for the purpose of assigning electronic transitions the general labels Ru(dπ) and diox($3b_1$) are used to designate orbitals of mainly metal and mainly dioxolene ($3b_1$) origin, respectively (see Table VIII and discussion below).

Table VIII. Summary of Electronic Spectroscopic Assignments

oxidation state	species[a]	wavelength region (nm)	assignment
R2	$[Ru^{II}(bpy)(cat)_2]^{2-}$	700–900	cat($3b_1$) → bpy(π_1^*)
			Ru(dπ) → bpy(π_1^*)
		500	Ru(dπ) → bpy(π_2^*)
R1	$[Ru^{III}(bpy)(cat)_2]^-$	800–900	cat($3b_1$) → bpy(π_1^*)
		700	cat($3b_1$) → Ru(dπ)(t_{2g}^5)
S	$Ru^{II}(bpy)(sq)_2$	900–1200	Ru(dπ) → sq($3b_1$)
		600	sq(n) → sq($3b_1$)
		500	Ru(dπ) → bpy(π_1^*)
O1	$[Ru^{II}(bpy)(sq)(q)]^+$	720–800	Ru(dπ) → diox($3b_1$)
		500–560	diox(n) → diox($3b_1$)

[a] The dominant oxidation state is cited for R1, S, and O1 for ease of assigning the spectra.

Electronic Structural Assignments. Species R2. These highly air-sensitive compounds were not isolated from solution; they are characterized by their electronic spectra and redox potentials. Referring to the possible electronic structures described above, reduction of the bipyridine ligand (R2,b) can be eliminated with three arguments: (a) the potential (V) is insufficiently negative,[70] (b) the pyridine series[42] has the R1/R2 couple in the same region, (c) there are no low lying absorption bands typical of a bpy$^-$ ion.[71] Thus R2 complexes are regarded as **$[Ru^{II}(bpy)(cat)_2]^{2-}$**.

There should be no low-energy charge transfer between metal and catechol. A low-energy Ru(dπ) → bpy(π_1^*) is expected, and possibly a low-energy ILCT transition from catecholate ($3b_1$) → bpy(π_1^*). The overall band envelope looks very similar to that in $Ru^{II}(bpy)_2$(DTBCat) (**5**,**R1**),[4] and the broad absorption at 700–900 nm is similarly assigned to both Ru(dπ) → bpy(π_1^*) and cat($3b_1$) → bpy(π_1^*). The bpy complex shows a band near 500 nm which is absent from the *trans*-R-py series and may contain Ru(dπ) → bpy(π_2^*). Both these Ru(dπ) → bpy(π^*) MLCT transitions lie lower in energy than in **5**,**R1** as expected on replacement of a bpy by DTBCat.

Species R1. The uppermost of the five orbitals discussed above will contain one unpaired electron. Visible region electronic transitions, other than those to bipyridine, will probably terminate on this orbital. Since these transitions shift to the blue with increasing acceptor character of the dioxolene ligand (Table VI), i.e., behave as LMCT transitions,[72] the inference is that the uppermost orbital has significant d character. On this evidence, R1 must have a major contribution from **$[Ru^{III}(bpy)(cat)_2]^-$**.

The Ru($3d_{5/2}$) PES core energy (Table V) appears consistent with the presence of Ru(II). However, the PES data do not exclude Ru(III) since the *trans*-[Ru(3-Clpy)$_2$(DTBCat)$_2$]$^-$ R1 species, which, from ESR evidence, undoubtedly contains Ru(III), has a binding energy of 281.4 eV,[42] within the Ru(II) range, the core energy probably being depressed because of the inductive

(69) Gordon, D. J.; Fenske, R. F. *Inorg. Chem.* **1982**, *21*, 2907, 2916.
(70) Dodsworth, E. S.; Lever, A. B. P. *Chem. Phys. Lett.* **1986**, *124*, 152.
(71) Heath, G. A.; Yellowlees, L. J.; Braterman, P. S. *J. Chem. Soc. Chem. Commun.* **1981**, 287.
(72) Lever, A. B. P. *Inorganic Electronic Spectroscopy*, 2nd Ed.; Elsevier Science Publishers: New York, 1984.

effect of the DTBCat ligands. The ESR spectra of **1,R1** and **2,R1** (Table III) give g values very close to the free radical value of 2, but their axial symmetry at low temperature suggests a significant contribution from Ru(III). The FTIR data are inconclusive, showing a typical catechol ν(C–O) around 1250 cm^{-1} and a strong band at 1415 cm^{-1} (Table IV) which could be either the expected catechol ring stretching mode, occurring at a similar frequency to that in the $Ru(bpy)_2(cat)$ series or the ν(C–O) of a coordinated semiquinone. The latter could only occur in a localized (Class I[73]) mixed-valence system, $[\mathbf{Ru^{II}(bpy)(sq)(cat)}]^+$, since in a delocalized (class IIIa) system an average of sq and cat ν(C–O) frequencies would be expected. Localized configurations are excluded by the five orbital model.

Finally, the substituent dependence of the R1/R2 couple (V) (Table II) is too small to be associated with a purely sq/cat redox process, and too large for a Ru(III)/Ru(II) couple. Thus this redox process probably involves both metal and ligand.

The electronic spectrum of R1 is most easily interpreted on the basis of the formula $[\mathbf{Ru^{III}(bpy)(cat)_2}]^+$. The strong band at around 700 nm is assigned primarily as $cat(3b_1) \rightarrow Ru(III)(t_{2g}^5)$ LMCT. A CT band, which can only be cat → Ru(III), is observed in a similar position in $[Ru^{III}(NH_3)_5(Cat)]^{+}$.[46] The broad, lower energy band is probably $cat(3b_1) \rightarrow bpy(\pi_1^*)$; this is also expected to blue shift as the catechol becomes a better electron acceptor. If the R1 species were deemed to exist purely in the $[\mathbf{Ru^{II}(bpy)(sq)(cat)}]^+$ form, then an intense $Ru(d\pi) \rightarrow sq(3b_1)$ transition, analogous to those in S and $[Ru(bpy)_2(sq)]^+$, would be expected to occur in the NIR below 950 nm; such a transition is not observed.

Thus the data can be explained in terms of an effective ruthenium oxidation state between Ru(II) and Ru(III) but closer to Ru(III). In valence bond terminology R1 is predominantly $[\mathbf{Ru^{III}(bpy)(cat)_2}]^-$ but with a resonance contribution from $[\mathbf{Ru^{II}(bpy)(cat)(sq)}]^+$.

Species S. Since these species are diamagnetic, the separation of the ligand a and b combinations must be great enough to cause spin pairing in the lower energy combination. The uppermost level is now empty (LUMO), and the five orbital model predicts that it has more ligand character (Figure 6) than in R1, and therefore that the species should be closer to Ru(II) in character. The X-ray structure of **2,S**[43] shows equivalent C–O distances (Table I) intermediate between those expected for sq and cat ligands.[19] Moreover the small thermal ellipsoids, elongated away from the C–O bond axes, indicate that the X-ray structure is not disordered. Evidently the dioxolene ligands are equivalent and intermediate between the catecholate and semiquinone forms. The PES data (Table V) for **1,S** and **2,S** are indicative of Ru(II), though **2,S** has a higher binding energy, probably reflecting the less basic dioxolene ligands.

The FTIR spectra (Table IV) are difficult to interpret. As the bond lengths in **2,S** are midway between those of catechol and semiquinone the C–O stretch would be expected (naively) to lie between 1250 and 1450 cm^{-1}. Species **2,S** shows a strong band in this region, at 1414 cm^{-1}, but the other complexes do not. The strongest bands in the spectra (1100–1200-cm^{-1} region) are too low in frequency for a simple assignment as ν(C–O), since this would imply (taking a simplified view) a C–O bond weaker than the single C–O bond of a coordinated catechol. However, the recent observation of similar bands in copper(II) semiquinone complexes[32] suggests that at least one ligand approximates to a semiquinone. The unusual FTIR spectra probably result from the low symmetry of these molecules, the covalency, and the extensive coupling expected between the various vibrational modes of the ligands[54] and between the three ligands via the ruthenium.

The electronic spectra are typified by a strong band in the NIR (see Figure 5), with a well defined lower energy shoulder or peak. Both the high intensity and narrow width of the NIR band are inconsistent with this absorption being due to intervalence (cat → sq) transitions.[16,44] The peak is very similar to NIR absorption in the spectrum of $[Ru^{II}(bpy)_2(DTBSq)]^+$ (**5,S**)[4] and is similarly assigned to $Ru(d\pi) \rightarrow sq(3b_1)$. Accordingly, there is a small red shift upon replacement of DTBSq by TClSq (Table VI). In the C_2 symmetry, transitions to L(a,b) from all three d orbitals are allowed, and therefore the two components of the NIR band probably reflect the d orbital splitting.

In the visible region there is a strong band near 600 nm and a weaker shoulder or peak near 500 nm. Ru(II)–bpy complexes show a $Ru(d\pi) \rightarrow bpy(\pi_1^*)$ transition with a molar absorption coefficient of approximately 4000 L mol^{-1} cm^{-1} per bpy ligand,[72] thus the 600-nm band is too strong to be so assigned, whereas the weaker band has approximately the expected intensity. In the rR spectrum of **1,S** bpy vibrations are enhanced when irradiating into the weaker band near 500 nm (and similarly for the 450-nm band of **3,S**) (Table VII). The frequencies agree well with the rR spectrum of the $[Ru(bpy)_3]^{2+}$ cation.[74] The weaker visible region band is then identified as $Ru(d\pi) \rightarrow bpy(\pi_1^*)$, an assignment supported by its appearance at roughly the expected energy, calculated by extrapolating from $[Ru(bpy)_3]^{2+}$ and $[Ru(bpy)_2(DTBSq)]^+$. This transition shifts to the blue when DTBCat is replaced by TClCat, consistent with some stabilization of the ruthenium d orbitals.

There remains the assignment of the strong 600-nm band. The rR data for irradiation at 570 nm show significant enhancement of vibrations which can be assigned to Ru–O stretching modes and deformation modes of the dioxolene ligand or the chelate ring.[47] Thus the 600-nm band is associated with the dioxolene rather than the bipyridine ligand. This conclusion also follows from the presence of a similar band in the spectra of the *cis*-$(R\text{-}py)_2Ru(diox)_2$ S species.[42] Two possible assignments can be considered. The first is a second MLCT transition similar to the NIR band (since the intensities are comparable) arising from a large splitting of the d ("t_{2g}") orbitals. Such a splitting (~6000 cm^{-1}) is unlikely as there is no bonding mechanism to discriminate between the three d orbitals to such an extent.

Alternatively, the transition may be related to the internal semiquinone, $n \rightarrow \pi^*$, transition which occurs in this region in the free ligand.[10] The oxygen lone pair orbital combinations span (2a + 2b) and may therefore mix with the ruthenium d orbitals; the relatively high intensity of this transition and the rR data require that the $n \rightarrow \pi^*$ transition have some $\pi \rightarrow \pi^*$ Ru–O character. This assignment is supported by the small blue shift that occurs on replacement of DTBDiox by TClDiox, consistent with some LMCT character. The transition is effectively from the lone pair of one semiquinone to the π^* of the other, the latter being strongly mixed with the metal orbitals. This transition is never observed as a prominent feature in the spectra of monosemiquinone metal complexes[4,53] or in the *trans*-$(R\text{-}py)_2Ru(diox)_2$ S species[42] because the forbidden character (no overlap to first order) of the $n \rightarrow \pi^*$ cannot be overcome in D_{2h} symmetry. In *cis*-bis-semiquinone species, this transition is strong only when there is significant metal–semiquinone mixing, for example in Cr(III) complexes.[11,14] In the absence of such mixing (e.g., in complexes of Mn, Fe, Co, and Ni[13,16,44]), the transition remains fairly localized and hence weak.

The S species are therefore best regarded as $\mathbf{Ru^{II}(bpy)(sq)_2}$, with significant mixing of metal and ligand orbitals, through Ru-sq π back-bonding, causing elongation of the C–O bonds. The R1 to S oxidation involves conversion of two mainly catecholate ligands to two mainly semiquinone ligands; the large shift in the potential of this couple upon replacement of DTBCat by TClCat is consistent with this conclusion.

Species O1. The upper two orbitals should now be mainly ligand in character and contain one electron. Thus the effective oxidation state lies between Ru(II) and Ru(III) but much closer to the former. The formulation $[\mathbf{Ru^{II}(bpy)(sq)(q)}]^+$ must, in this model, have equivalent (delocalized) dioxolene ligands, i.e., a class III mixed-valence species.[73]

The PES $Ru(3d_{5/2})$ binding energy lies on the boundary between "normal" Ru(II) and Ru(III) (Table V). The FTIR data (Table

(73) Robin, M. B.; Day, P. *Adv. Inorg. Chem. Radiochem.* **1967**, *10*, 248.

(74) Dallinger, R. F.; Woodruff, W. H. *J. Am. Chem. Soc.* **1979**, *101*, 4391.

IV, Figure 4C) do not show clearly the presence of either quinone or semiquinone. The magnetic data and ESR spectrum (Table III) indicate the presence of only one unpaired electron and exclude an uncoupled $[\mathbf{Ru^{III}(bpy)(sq)_2}]^+$ formulation. The ESR spectrum is consistent with a free radical but with a very small g anisotropy which is the opposite of that typically observed for axial Ru(III)[50] and also for reduced bpy in $[Ru(bpy)_3]^{(2-n)+}$[51] but the same as in $[Ru(bpy)_2(DTBSq)]^+$.[4] The proportion of Ru(III) in O1 is predicted, by the five orbital model, to be less than in R1, and this is confirmed by the ESR data where the g anisotropy is considerably smaller in O1 than in R1.

The electronic spectra (Table VI) show two intense bands in the visible region, near 720 and 545 nm. Both shift to the red as the ligand becomes more electron withdrawing, consistent with MLCT, confirming that the LUMO is now mainly ligand in character. These two bands are comparable in intensity and in energy separation with the strong NIR and visible region bands in the S complexes, which suggests that they may have similar assignments. As in the S series, the higher energy band is present only very weakly (at 520–580 nm) in the *trans*-pyridine O1 series but more strongly in the *cis*-pyridine series.[42] This evidence supports the formulation $[\mathbf{Ru^{II}(bpy)(sq)(q)}]^+$.

RR spectra (Table VII) in the visible region show enhancement of mainly low-energy modes, corresponding to dioxolene or chelate ring deformations and ν(Ru–O).[47] Data have not been obtained for direct excitation into the 720-nm band, but it appears (from excitation at 620 nm into the tail of this band) that the same frequencies are enhanced in both transitions. This precludes assignment of the transitions as localized $Ru(d\pi) \rightarrow q(3b_1)$ and $Ru(d\pi) \rightarrow sq(3b_1)$, but it is consistent with assignments similar to those given above for S (see Table VIII). An additional transition is also expected from $Ru(d\pi)$ to the partly occupied lower ligand combination orbital. This may account for the absorption between the two peaks in the visible region. The band at 400 nm almost certainly involves $Ru(d\pi) \rightarrow bpy(\pi_1^*)$, shifted to higher energy from the S species due to stabilization of the Ru d orbitals.

Species O2. The trends discussed above and the five orbital model predict that O2 will be $[\mathbf{Ru^{II}(bpy)(q)_2}]^{2+}$, but there are insufficient data available to confirm this.

Summary and Conclusions

The electronic structures of the various species may be represented as

R2 $[Ru^{II}(bpy)(cat)_2]^{2-}$

R1 $[Ru^{III}(bpy)(cat)_2]^- \leftrightarrow [Ru^{II}(bpy)(cat)(sq)]^-$

S $Ru^{II}(bpy)(sq)_2 \leftrightarrow Ru^{III}(bpy)(cat)(sq)$

O1 $[Ru^{II}(bpy)(sq)(q)]^+ \leftrightarrow [Ru^{III}(bpy)(sq)_2]^+$

O2 $[Ru^{II}(bpy)(q)_2]^{2+}$

with the first cited species being dominant and with extensive overlap between the ruthenium d orbitals and dioxolene frontier orbitals, i.e., extensively delocalized. There has been no substantial evidence previously for delocalization to this extent in dioxolene complexes;[3] these data therefore represent the first such detailed evidence for this behavior.

The various techniques undertaken here all provide a measure of the effective oxidation state, but there are frequently ambiguities in interpretation. PES in particular was not as useful as we had hoped since it measures the net charge felt by inner electrons, which in these complexes strongly reflects the basicity of the ligands. For localized systems FTIR usually provides a useful guide to the oxidation state of the dioxolene ligand. In delocalized mixed-valence systems it is potentially useful but requires full analysis of the spectra. ESR and electronic spectra, especially when supported by resonance Raman spectroscopy, provide the most accurate representations. A more detailed MO analysis of the various members of these redox series is in hand and should give further clarification.

Acknowledgments. We are indebted to the Natural Science and Engineering Research Council (NSERC) (Ottawa) and the Office of Naval Research (Washington) for financial support and to Johnson-Matthey Ltd. for loans of ruthenium(III) chloride. We also thank Professor C. G. Pierpont for advance information on the crystal structure of $Ru(bpy)(Diox)_2$ and Professors L. K. Thompson and D. J. Stufkens for the magnetism and resonance Raman measurements, respectively.

Registry No. 1,O1, 116926-58-0; **1,O2**, 116926-70-6; **1,R1**, 116926-62-6; **1,R2**, 116926-64-8; **1,S**, 116926-63-7; **2,O1**, 116926-68-2; **2,R1**, 116926-60-4; **2,S**, 116926-55-7; **3,O1**, 116926-69-3; **3,R1**, 116926-66-0; **3,R2**, 116926-65-9; **3,S**, 116926-56-8; **5,S**, 116926-61-5; $Ru(bpy)Cl_3$, 69141-04-4; $AgClO_4$, 7783-93-9; $AgPF_6$, 26042-63-7; 3,4,5,6-tetrachlorocatechol, 1198-55-6; *o*-chloranil, 2435-53-2; cobaltocene, 1277-43-6.